



## **Analysis and design of steel plate shear walls with column restrainers**

M.A. Amer<sup>1</sup>, S.S. Safar<sup>2</sup>, B.E Machaly<sup>3</sup>

### **Abstract**

Previous research work on steel plate shear walls revealed that more than 60% of the shear strength of such systems was attributed to diagonal tension forces supported by in-fill plate after buckling. Therefore current specifications stipulated minimum inertia for columns to develop uniform diagonal tension field and achieve full yielding of the in-fill plate at ultimate load. However, previous numerical research work revealed that such inertia requirement might not be sufficient to develop full yielding of in-fill plate in the bottom panel when the tensile strength of in-fill plate and/or number of floors increased. Hence, theoretical shear strength of the wall might not be achieved. In this paper, the effect of using column restrainers on the behavior and strength of steel plate shear walls was investigated by the finite element method. Non-linear pushover analysis results of more than eighty column-restrained shear walls revealed that the use of column restrainers developed uniform diagonal tension field in the in-fill plate in all panels, accelerated yielding of in-fill plate at a drift of not more than 2.5%, and prevented formation of plastic hinges near mid span of first story columns when tensile strength of in-fill plate and/or number of floors were increased. Since column in-ward deflections between floor beams were almost eliminated when column restrainers were used, rigidity requirements of columns in column-restrained walls were reduced compared to unrestrained walls. Numerical results were used to express the ultimate shear strength of column-restrained steel plate shear walls in-terms of geometric and material properties of the wall and to propose new design requirements for columns and restrainers of such systems.

### **1. Introduction**

Typical steel plate shear walls, SPSWs, are composed of infill plate surrounded by beams and columns designated as boundary frame elements as shown in Fig 1. The infill plate is slender, thus principal compressive stresses due to shear cause the plate to buckle and form diagonal tension folds at ultimate load (Amer 2014, Berman 2003). SPSWs were conventionally designed (Berman 2003) using an analytical approach at which in-fill plates were replaced by series of strips inclined at an angle  $\alpha$  with the vertical. Using elastic strain energy formulation of an equivalent story brace, the angle  $\alpha$  was expressed in terms of wall parameters as follows:

---

<sup>1</sup> PhD candidate, Cairo University, <mamer7@yahoo.com>

<sup>2</sup> Associate Professor, American University in Cairo, <ssafar@aucegypt.edu>

<sup>3</sup> Professor, Cairo University, <machaly2000@hotmail.com>

$$\tan^4(\alpha) = \frac{1 + \frac{t_p L}{2A_c}}{1 + t_p h_p \left( \frac{1}{A_b} + \frac{h_p^3}{360I_c L} \right)} \quad (1)$$

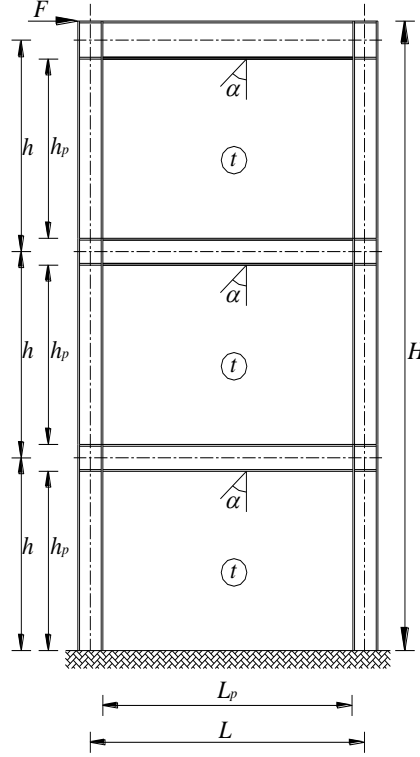


Figure 1: Geometric configurations of a typical three stories-single bay SPSW

where  $t_p$  is the thickness of infill plate,  $L$  is the width measured between centerlines of columns,  $h_p$  is the height of infill plate per floor,  $A_c$  and  $A_b$  is the cross sectional area of columns and beams surrounding infill plate; respectively, and  $I_c$  is the in-plane moment of inertia of columns cross section. The ultimate shear strength of SPSW,  $V_s$ , was theoretically computed as the sum of base shear supported by infill plate,  $V_p$ , and that supported by boundary frame elements,  $V_f$  as follows:

$$V_s = V_p + V_f \quad (2)$$

For multistory SPSW with identical infill plate thicknesses in all floors,  $V_p$  was determined by plastic analysis assuming that infill plates in all stories were fully yielded as follows (Berman 2003):

$$V_p = \frac{1}{2} F_{yp} t_p L_p \sin(2\alpha) \quad (3)$$

where  $F_{yp}$  and  $L_p$  is the yield strength and width of infill plate; respectively. The base shear supported by boundary frame elements with rigid beam-to-column connections and compact beams and columns was computed by plastic analysis assuming uniform yielding mechanism as follows (Berman 2003):

$$V_f = \frac{\sum M_p}{H} \quad (4)$$

where  $\sum Mp$  is the sum of plastic moments at ends of all beams, and  $H$  is the overall height of the wall. Eqs (1) to (3) were adopted by AISC specifications (AISC 2005) and Canadian specifications (CSA 2001) to compute ultimate shear strength of SPSW after dividing Eq (3) by an over-strength factor of 1.2. Based on Wagner flange flexibility parameter that was derived for plate girders, the AISC 341-05 and CSA S16-01 stipulated minimum inertia,  $I_{co}$ , for columns of SPSWs to develop uniform diagonal tension field in the in-fill plate and achieve full yielding capacity of in-fill plates as follows:

$$I_{co} \geq 0.00307 \frac{t_p h^4}{L} \quad (5)$$

Experimental and numerical research programs conducted by Driver 1997, Berman 2003, Behbahanifard 2003, Park 2007, and Choi 2008 and 2009 elaborated on the behavior and strength of SPSWs. Fewer tests, however, were conducted on CR-SPSW. Chao 2010 conducted full scale test on two story-single bay SPSWs and CR-SPSWs depicted in Fig 2. The in-fill plate in all specimens was composed of mild steel with  $F_{yp}$  of 195 MPa whereas the boundary elements were composed of high grade steel with  $F_{yf}$  ranging from 358 to 492 MPa (Chao 2010). The testing program was established to monitor the hysteresis behavior, shear strength of narrow width SPSWs and the effect of using column-restrainers, reduced beams and columns section, RBS and RCS; respectively (see Fig 2). Table 1 lists the geometric dimensions and designation of the four tested specimens. Results indicated that specimen N with strong column ( $I_c = 1.2 I_{co}$ ) provided the highest shear strength compared to other specimens. The shear strength of wall was reduced by 27% when weak column was used ( $I_c = 0.78 I_{co}$ ) in specimen S and plastic hinges were formed above base connection of first story columns at collapse. On the other hand, the use of column-restrainers in specimens RS and CY with  $I_c = 0.78 I_{co}$  stabilized the hysteresis behavior and shifted plastic hinges in the first story columns towards base connection. The effect of using RBS and/or RCS on behavior and strength of tested walls was minimal.

Table 1: Geometric dimensions of specimens tested by Chao 2010

No	Panel Dimensions (mm)					Column H ( $h_w \times b_f / t_w \times t_f$ )	Remarks
	$L_p$	$h_p$	$t_p$	$L_p/h_p$	$L_p/t_p$		
N	1790	2875	2.6	0.62	688	H(350x350 / 12x19)	RBS
S	1840	2875	2.6	0.64	707	H(300x300 / 10x15)	
RS	1840	2875	2.6	0.64	707	H(300x300 / 10x15)	Restrainers and RBS
CY	1840	2875	2.6	0.64	707	H(300x300 / 10x15)	Restrainers, RBS and RCS

In this paper, the ultimate shear strength of CR-SPSW was investigated by the finite element method. Numerical solution was verified by comparison to test results obtained by Chao 2010. The verified model was used to conduct push-over analysis on eighty two CR-SPSWs with wide variety of geometric and material properties. Numerical results were used to establish design expression and requirements for CR-SPSWs.

## 2. Finite Element Modeling and Verification

The finite element model of CR-SPSW was established by modeling in-fill plate, boundary elements and column-restrainers with iso-parametric finite strain shell element, SHELL 181, built in ANSYS element library (Desavlo 1989, Machaly 2012). SHELL 181 is a four noded element with six degrees of freedom per node that is well-suited for large rotation and/or large strain nonlinear applications. Nodes at column base were restrained against translation and

rotation to mimic fixed support whereas nodes at beam-to-column connections were restrained against out-of-plane displacement to resemble out-of plane bracing provided by floors. The material model of steel was assumed to be bilinear isotropic with non-zero tangent modulus to avoid numerical instability. Von-Mises yield criterion was adopted to model yielding of steel.

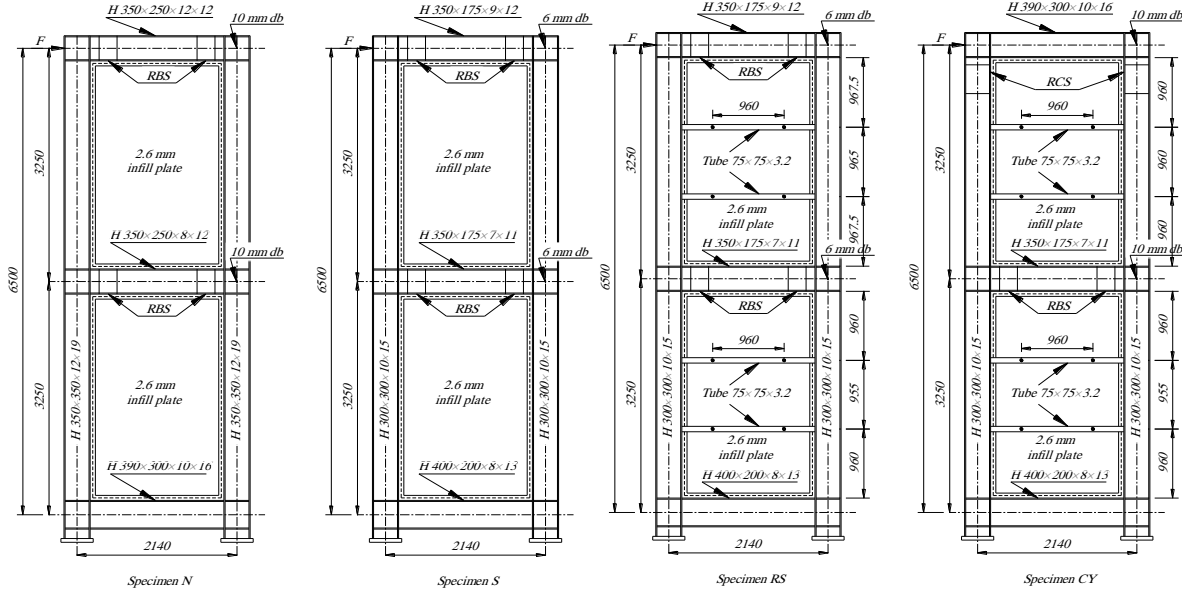


Figure 2: Specimens tested by Chao 2010

Pushover analysis conducted herein was essentially non-linear static analysis at which loading was applied as progressively increasing lateral displacement at the level of top beam. The converged solution after each displacement increment was obtained by iterations using the Full Newton-Raphson technique (Desalvo 1989). The solution was terminated at the first limit load or when the drift of the wall reached 2.5% from total height,  $H$ . Due to the high non-linear nature of the problem, severe convergence difficulties could occur due to large out-of-plane displacements of in-fill plate. Therefore a special nonlinear stabilization technique was used by adding an artificial damper at each node with a small damping factor of  $5 \times 10^{-6}$  (Desalvo 1989). The force in the damper was proportional to nodal displacement per load increment. Therefore the node that tended to be unstable had large displacement increment causing large damping force that reduced the displacement and stabilized the model. On the other hand, the effect of damping forces was minimal on stable nodes with small displacement increment (Desalvo 1989).

The finite element model was verified by solving shear walls tested by Chao et al (see Table 1 and Fig 2). Contour plot of Von-Mises stresses at ultimate load of specimen N (see Fig 3) revealed that in-fill plate was fully yielded when strong column ( $I_c = 1.2 I_{co}$ ) was used. Although RBS were utilized, boundary frame elements collapsed by plastic hinging at base connections of columns (see Fig 4), plastic hinging at ends of top beam, and column web yielding at top beam-to-column connection. When weak column ( $I_c = 0.78 I_{co}$ ) was used in specimen S, the in-fill plate in the bottom panel did not achieve full yielding at ultimate load (see Fig 5). On the other hand, plastic hinge at column base was shifted towards mid-height (see Fig 6) and plastic hinges at the end of top beam were eliminated. Similar to test results, the numerical solution predicted a reduction in shear strength of specimen S compared to that of specimen N by 25%.

When column restrainers were used in specimens RS and CY with weak columns ( $I_c = 0.78 I_{co}$ ), in-fill plate was fully yielded as depicted in Figs 7 and 8. On the other hand, plastic hinges in first story columns were shifted towards base connection. Collapse of boundary frame elements in specimens RS and CY was caused by plastic hinging at ends of beams and column web yielding at the top beam-to-column connection. Similar to test results it was shown that the use of RCS did not alter significantly the overall behavior of specimen CY compared to specimen RS except for the formation of localized yielded zones in column flanges at the reduced column section (see Fig 8).

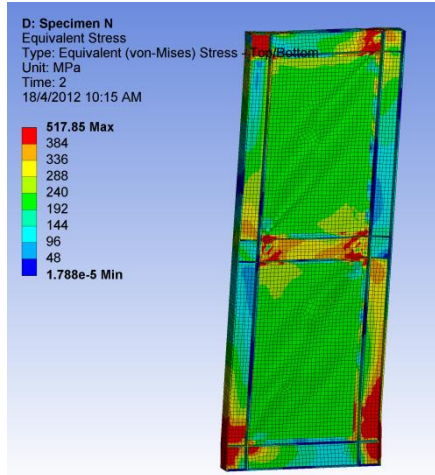
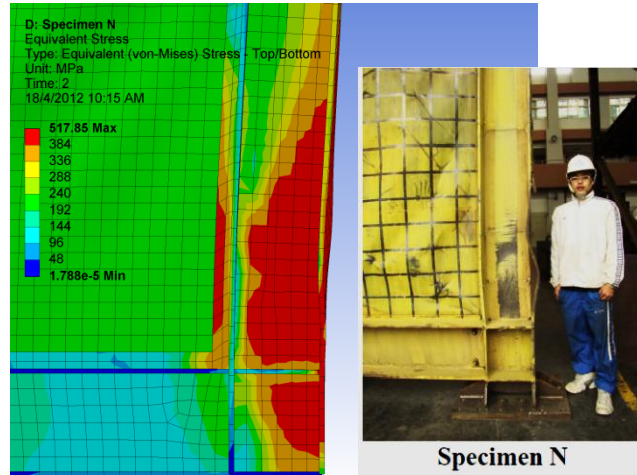


Figure 3: Von-Mises stresses (MPa) at Limit load, Specimen N



a) Finite Element      b) Test (Chao 2010)  
Figure 4: Plastic hinge at base connection, Specimen N

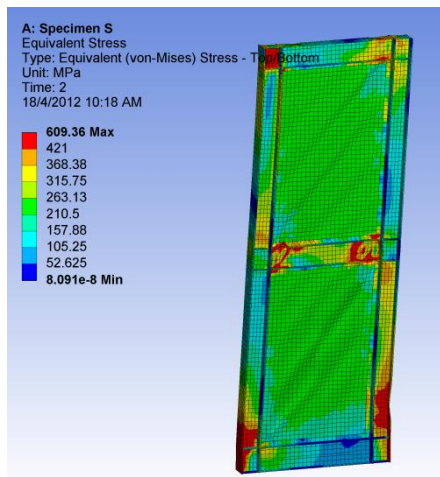
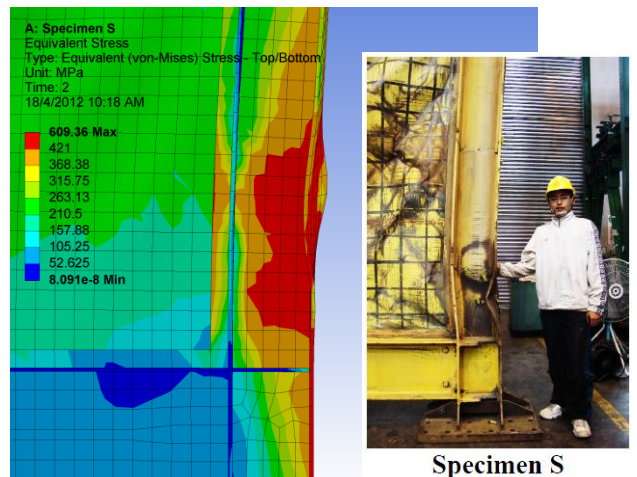


Figure 5: Von-Mises stresses (MPa) at Limit load, Specimen S.



a) Finite Element      b) Test (Chao 2010)  
Figure 6: Plastic hinge shifted upwards, Specimen S

Fig 9 shows that numerical push-over curves of all specimens enveloped hysteresis curves obtained by test (Chao 2010). The ultimate shear strength obtained numerically using push-over analysis predicted the maximum base shear obtained by test due to cyclic loading with a maximum difference of 8%. Although the addition of column restrainers did not alter the ultimate shear strength significantly, it caused full yielding of in-fill plate, limited yield zone in

first story columns close to base connections and stabilized the hysteresis behavior of the wall compared to identical unrestrained walls.

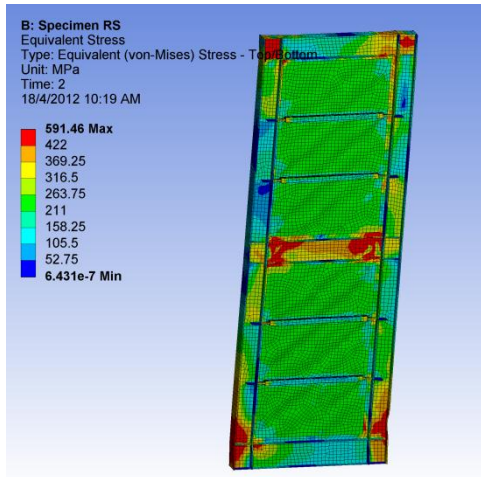


Figure 7: Von-Mises stresses (MPa) at limit load, Specimen RS

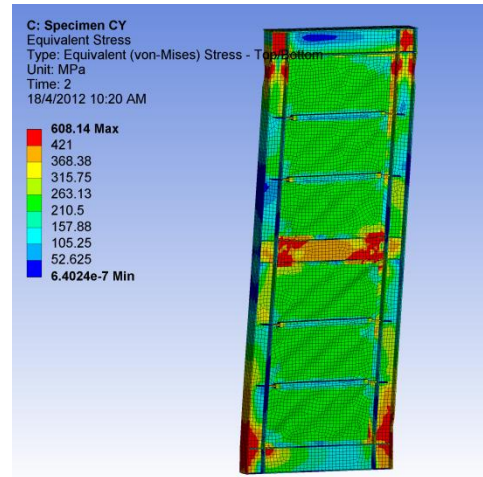


Figure 8: Von-Mises stresses (MPa) at limit load, Specimen CY

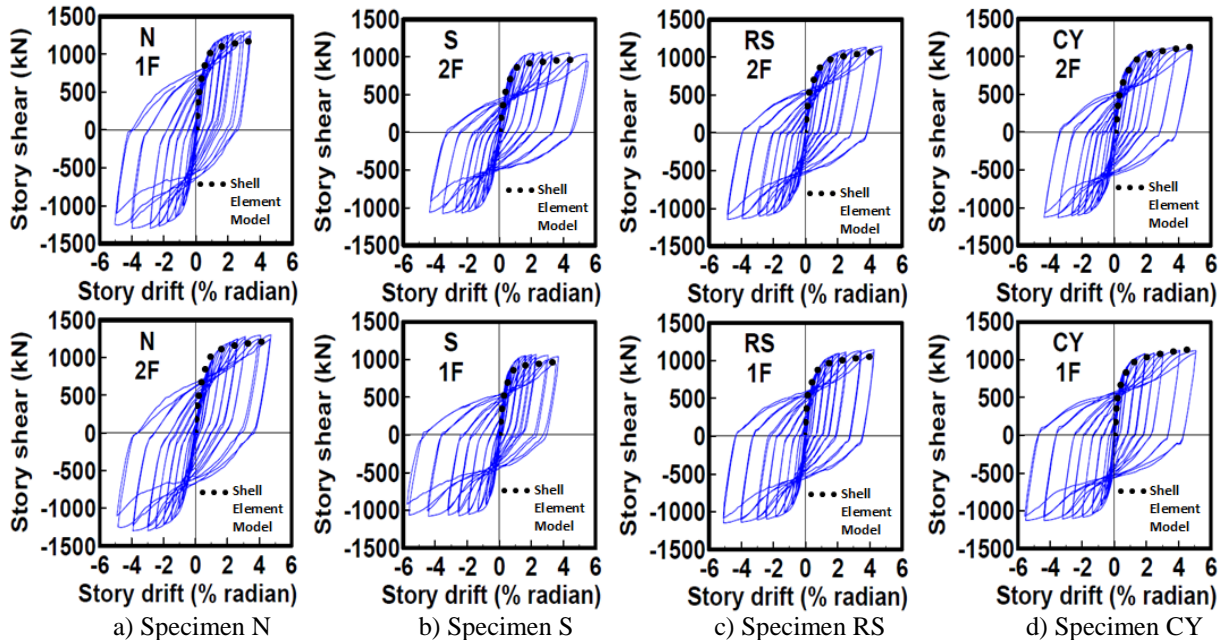


Figure 9: Comparison of numerical push-over curves to test hysteresis curves for specimens tested Chao 2010

### 3. Pushover Analysis of Unrestrained and Column-restrained SPSWs

In this section, the push over analysis of SPSWs with and without column restrainers was conducted to assess the effect of using column-restrainers on the behavior and shear strength of SPSWs. A three stories-single bay shear wall with plate width,  $L_p$ , of 4785 mm and plate height,  $h_p$ , of 3300 mm was proportioned using Eqs (1 to 4) to support a base shear of 5000 KN. The yield strengths of in-fill plate and boundary frame elements were assumed 280 MPa and 360 MPa; respectively. In-fill plates in all floors were assumed with identical thickness of 5 mm. Columns and beams were assumed rigidly connected whereas columns were fixed at the base.

Columns were composed of compact I-shaped section H(130x400/54x54) with inertia,  $I_c = 0.80 I_{co}$ , whereas floor beams were composed of compact I-shaped section H(320x330/18x48). To account for un-balanced tension forces applied on the top beam, the section of the top beam was assumed to provide 4 times the inertia and 1.33 times the area of that of typical intermediate beams. Column-restrainers were composed of compact plates welded to both sides of in-fill plates and were proportioned to support axial compression force resulting from the horizontal component of diagonal tension forces applied on columns assuming full yielding of the in-fill plate. Out-of-plane buckling length of column-restrainers was assumed  $0.75L_p$  to account for partial fixation of restrainers at columns.

Push-over analysis of the wall was repeated three times; without using column restrainers (i.e.  $n_r = 0$ ), using one column restrainer at mid-height of floor (i.e.  $n_r = 1$ ) and using two column restrainers at one-third and two-thirds of floor height (i.e.  $n_r = 2$ ). Fig 10 shows that the initial slope of pushover curves of SPSW was not altered when column-restrainers were introduced, however, the energy dissipated and shear strength of the wall slightly increased by 3%. The number of column-restrainers had minor effect on behavior and strength of the wall. The base shear supported by the infill plate,  $V_p$ , was computed numerically by summing the horizontal component of nodal forces at the base of the in-fill plate of the bottom panel at ultimate load. The ratio of  $V_p$  to that computed by plastic theory,  $V_{p(Theory)}$ , (Eq 3) represented the percentage of utilized tensile strength of in-fill plate. Table 2 shows that CR-SPSW utilized the full tensile strength of the in-fill plate whereas the base shear supported by boundary frame elements,  $V_f$ , decreased by 17% and did not exceed 67% from that computed by plastic analysis assuming uniform mechanism,  $V_{f(Theory)}$ , (Eq 4). Hence, the use of column restrainers utilized the full tensile strength of in-fill plate and reduced internal forces in boundary frame elements at a drift of not more than 2.5% such that the base shear supported by the in-fill plate constituted more than 70% of the wall shear strength (see Table 2). Distribution of angle of inclination of principal tensile stresses on left and right columns in Fig 11 revealed that the use of column restrainers slightly increased  $\alpha$  compared to theory (Eq 1). Therefore, the magnitude of  $V_p$  computed numerically slightly exceeded  $V_{p(Theory)}$  (Eq 3).

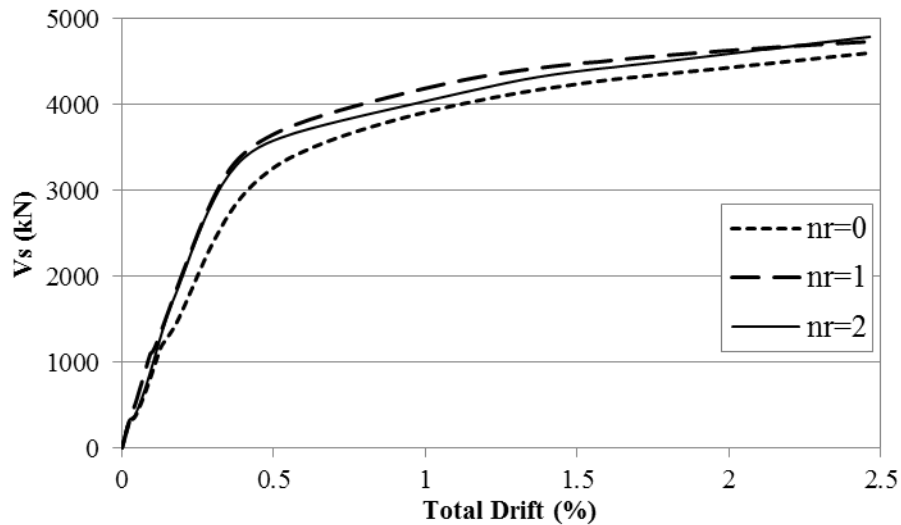


Figure 10: Comparison of push-over curves of unrestrained and column-restrained SPSWs



Table 2: Effect of column-restrainers on  $V_p$  and  $V_f$

Number of column-restrainers per floor, $n_r$	$V_p/V_{p(Theory)}$	$V_f/V_{f(Theory)}$	$V_s/V_{s(Theory)}$	$V_p/V_s$
0	0.92	0.80	0.87	0.66
1	1.03	0.67	0.90	0.72
2	1.06	0.65	0.91	0.73

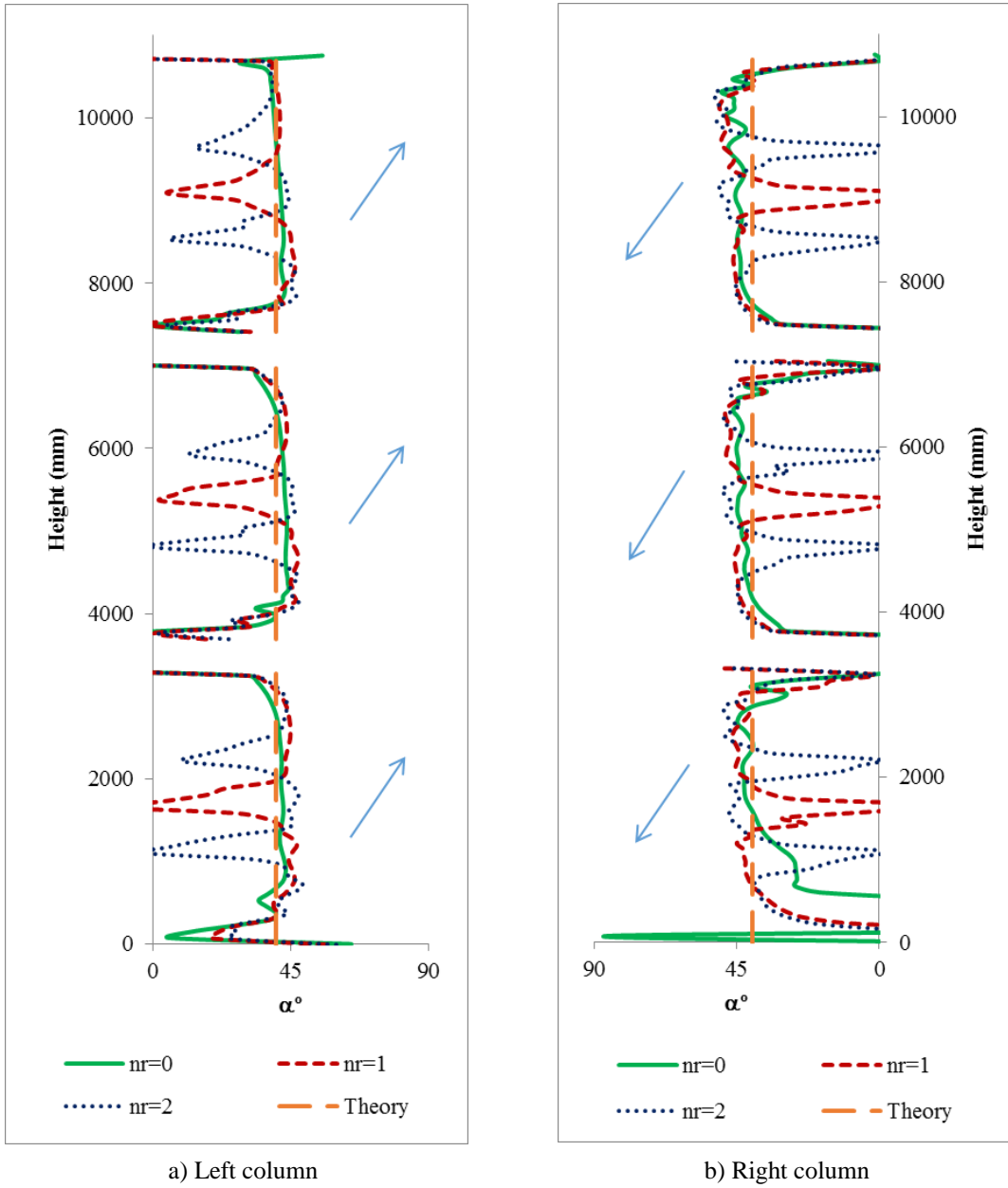


Figure 11: Distribution of the angle of inclination of principal tensile stresses,  $\alpha$ , on columns



#### 4. Parametric Analysis

The geometric and material properties of the ‘basic’ SPSW solved in Sec 3 were varied within practical limits as listed in Table 3. The variables considered in the parametric analysis were:  $h_p$ ,  $L_p$ ,  $t_p$ ,  $I_c$ ,  $F_{yp}$ ,  $F_{yf}$ ,  $A_c$ ,  $I_b$ ,  $A_b$ ,  $n_f$  and  $n_r$ . The parametric analysis was conducted by varying the magnitude of each parameter independently whereas the magnitudes of other parameters were kept unchanged. To facilitate generalizing results, the geometric and material variables of the wall were normalized as follows:  $I_c/I_b$ ,  $F_{yp}/F_{yf}$ ,  $t_p h_p/A_b$ ,  $t_p L_p/2A_c$  and  $A_c/A_{co}$  where  $A_{co}$  is the yield load area of the column defined (Amer 2014) as the area of the column at which the yield load capacity, i.e.  $A_{co}F_{yf}$ , equals to the sum of the theoretical vertical components of diagonal tension forces applied on columns and top beam (see Fig 12). For SPSWs with identical in-fill plate thickness in all floors,  $A_{co}$  was computed as follows:

$$A_{co} = \frac{(w_{cv} h_p n_f + 0.5 w_{bv} L_p)}{F_{yf}} \quad (6)$$

where  $w_{cv} = F_{yp} t_p \cos \alpha \sin \alpha$  is the vertical component of diagonal tension forces applied per unit length on columns, and  $w_{bv} = F_{yp} t_p \cos^2 \alpha$  is the vertical component of unbalanced diagonal tension forces applied per unit length on top beam (Amer 2014). The inertia and area of intermediate beams were related to top beam as assumed in Sec. 3.

Table 3: Limits of variables of SPSWs included in the parametric analysis

Variable Description	Symbol	Limits of Variable	
		Minimum	Maximum
In-fill plate height (mm)	$h_p$	2300	4800
In-fill plate width (mm)	$L_p$	1800	5300
In-fill plate thickness (mm)	$t_p$	3	7
Moment of inertia of columns (mm <sup>4</sup> )	$I_c$	3.8E+8	1.52E+10
Area of columns (mm <sup>2</sup> )	$A_c$	35000	90000
Moment of inertia of top beam (mm <sup>4</sup> )	$I_b$	2.29E+9	9.12E+9
Area of top beam (mm <sup>2</sup> )	$A_b$	50000	100000
Number of floors	$n_f$	2	6
Number of column-restrainers	$n_r$	0	2
Yield strength of in-fill plate (MPa)	$F_{yp}$	120	360
Yield strength of frame (MPa)	$F_{yf}$	260	960

#### 5. Discussion of Results

##### 5.1 Base shear supported by in-fill plate, $V_p$

Fig 13 shows that the use of column restrainers reduced column-inward deflections,  $\delta$ , between floor beams to less than 0.005 of  $h_p$ . Therefore  $V_p/V_{p(Theory)}$  was independent on  $\delta/h_p$  and exceeded 0.90 in CR-SPSWs. On the other hand,  $V_p/V_{p(Theory)}$  was inversely proportional to  $\delta/h_p$  in SPSWs. Fig 14 illustrates that the use of column restrainers reduced the area of columns required to achieve full yielding of in-fill plate. In SPSW,  $A_c$  was required to exceed  $2.5A_{co}$  to achieve more than 95% of tensile strength of in-fill plate. However, in CR-SPSWs, full yielding of in-fill plate was achieved at  $A_c = 1.7 A_{co}$ . Unlike SPSWs that required the increase of  $I_c$  to

multiples of  $I_{co}$  to increase  $V_p$ , the value of  $V_p/V_{p(Theory)}$  exceeded unity in CR-SPSW with  $I_c = 0.8 I_{co}$  and was independent on  $I_c/I_{co}$  as depicted in Fig 15.

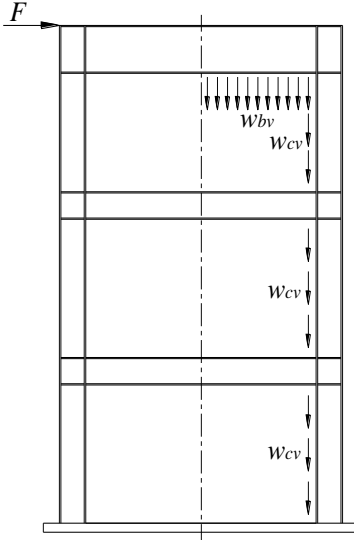


Figure 12: Vertical component of diagonal tension forces on right column of a typical SPSW

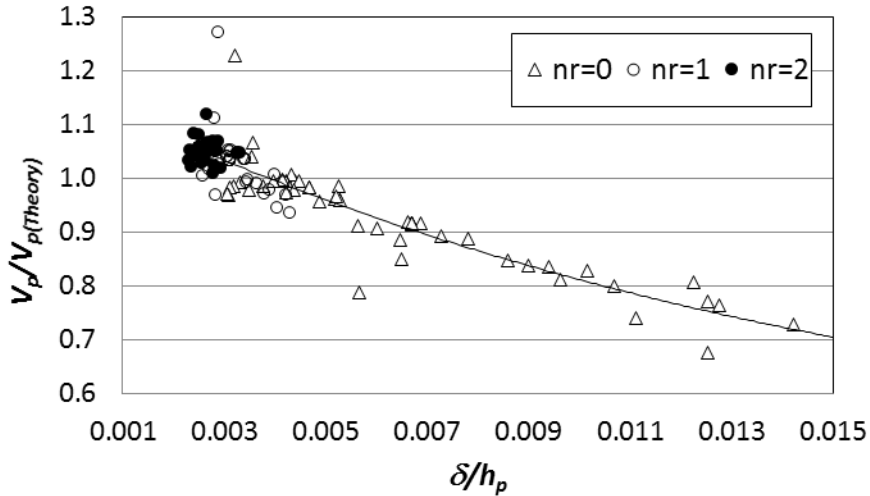


Figure 13: Relationship between column inward deflections on  $V_p/V_{p(Theory)}$  in SPSWs and CR-SPSWs

Fig 16 illustrates that the increase of  $F_{yp}/F_{yf}$  without respective increase in the axial and flexural rigidity of boundary frame elements reduced the base shear supported by in-fill plate. However, in CR-SPSWs,  $V_p/V_{p(Theory)}$  exceeded unity when  $F_{yp}/F_{yf} \leq 0.80$ . On the other hand, in SPSW,  $V_p/V_{p(Theory)}$  decreased when  $F_{yp}/F_{yf} > 0.60$ . Figs 17 and 18 illustrate that the use of column restrainers reduced  $A_b$  and  $A_c$  required to utilize the full yielding capacity of the infill plate. The value of  $V_p/V_{p(Theory)}$  exceeded unity when  $t_p h_p / A_b$  was less than 0.35 and 0.5 in CR-SPSW with  $n_r=1$  and 2; respectively. However, in SPSW,  $V_p/V_{p(Theory)}$  exceeded unity when  $t_p h_p / A_b$  was less than 0.25. Similarly, the value of  $V_p/V_{p(Theory)}$  exceeded unity when  $t_p L_c / 2A_c$  was less than 0.25 and 0.35 in CR-SPSW with  $n_r=1$  and 2; respectively. However, in SPSWs,  $V_p/V_{p(Theory)}$  reached unity when  $t_p L_c / 2A_c$  was reduced to 0.15. Fig 19 shows that the increase of number of floors

without respective increase in  $A_c$  and  $I_c$  reduced  $V_p/V_{p(Theory)}$  progressively in SPSW due to the magnification of column in-ward deflections. However, in CR-SPSW,  $V_p/V_{p(Theory)}$  was less dependent on  $n_f$  since column inward deflections were significantly reduced (see Fig 13). The value of  $V_p/V_{p(Theory)}$  exceeded 0.9 and 1.0 in five stories CR-SPSWs with  $n_r=1$  and 2; respectively compared to  $V_p/V_{p(Theory)}$  of 0.72 in identical SPSW.

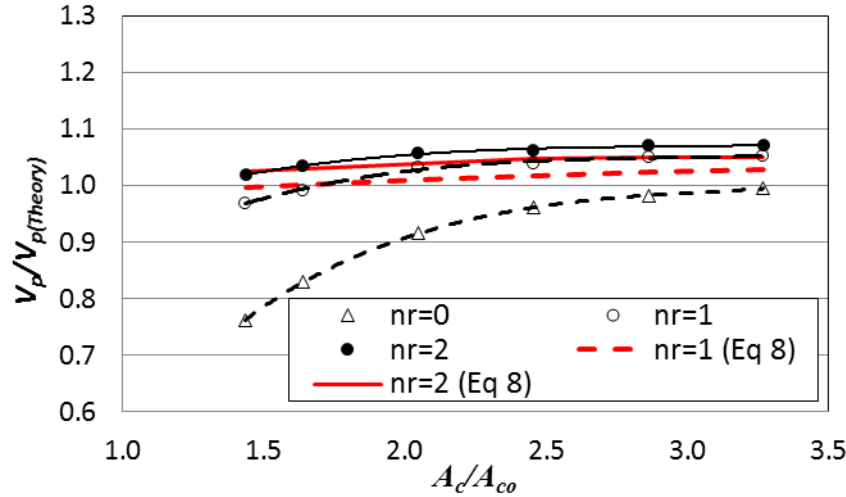


Figure 14: Effect of  $A_c/A_{co}$  on  $V_p/V_{p(Theory)}$

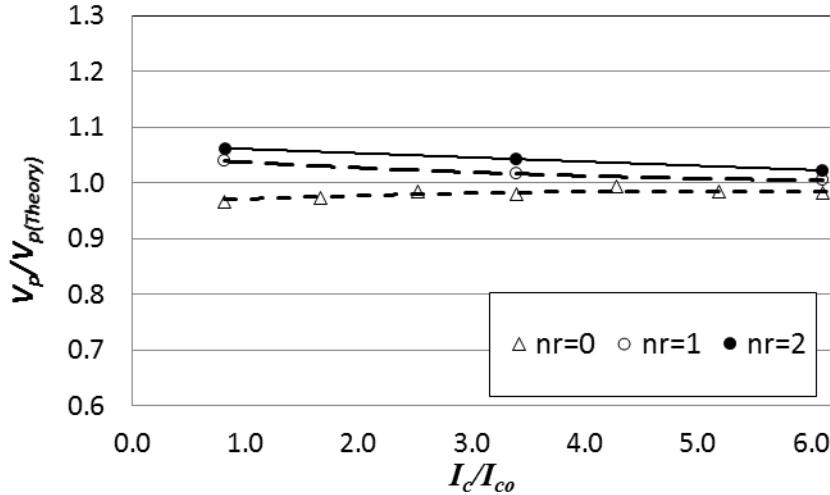


Figure 15: Effect of  $I_c/I_{co}$  on  $V_p/V_{p(Theory)}$

### 5.2 Base shear supported by boundary frame elements, $V_f$

Fig 20 showed that the use of restrainers accelerated the increase of  $V_f$  when  $A_c$  increased. In CR-SPSW, the value of  $V_f/V_{f(Theory)}$  increased proportionally with  $A_c$  when  $A_c/A_{co} \geq 1.5$ . However, in SPSW,  $V_f/V_{f(Theory)}$  started to increase with  $A_c$  when  $A_c/A_{co}$  exceeded 2.5. On the other hand, the value of  $V_f/V_{f(Theory)}$  reduced to 0.7 in CR-SPSW compared to a respective value of 0.8 in unrestrained SPSW when  $A_c/A_{co}$  was 2.5. Therefore the use of restrainers reduced the base shear supported by the frame at a given drift thus satisfied the elastic condition requirement for boundary frame elements stipulated by current codes (AISC 2005, CSA 2001).

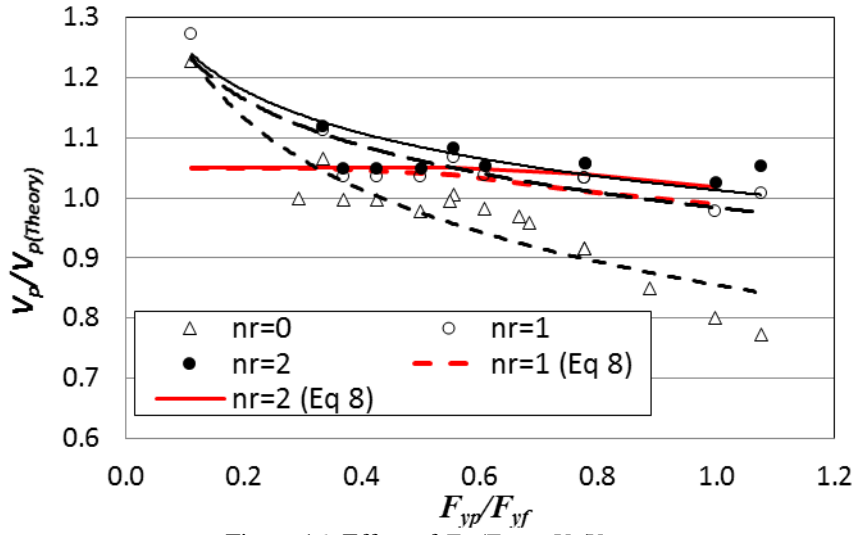


Figure 16: Effect of  $F_{yp}/F_{yf}$  on  $V_p/V_{p(Theory)}$

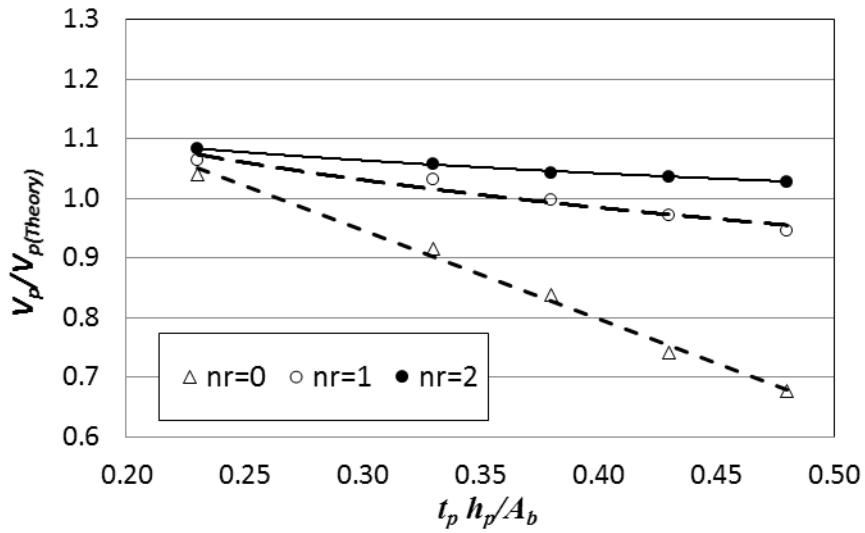


Figure 17: Effect of  $t_p h_p/A_b$  on  $V_p/V_{p(Theory)}$

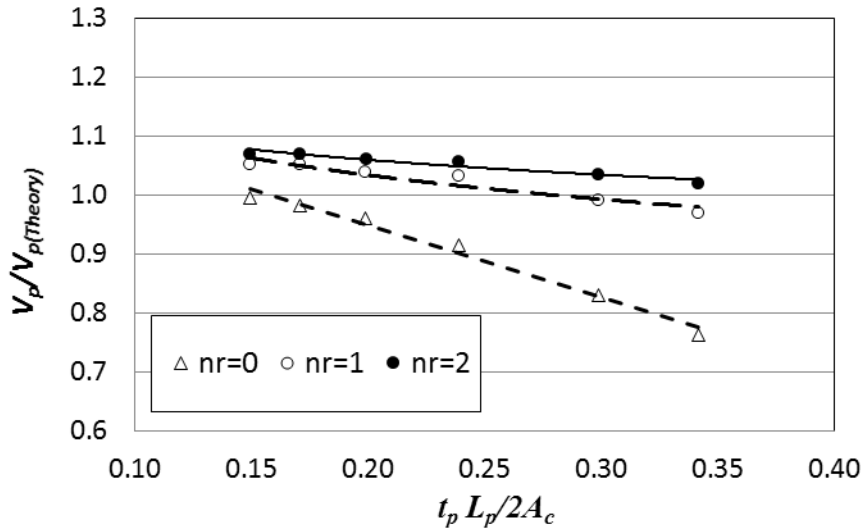


Figure 18: Effect of  $t_p L_p/2A_c$  on  $V_p/V_{p(Theory)}$

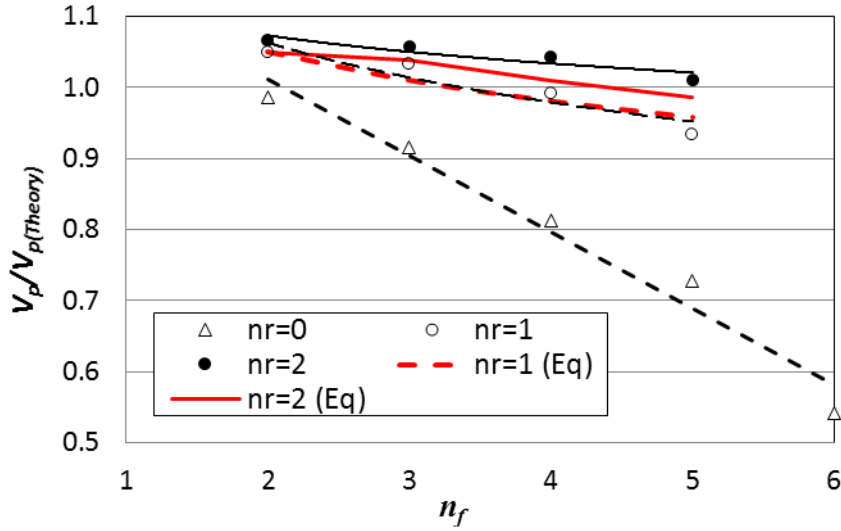


Figure 19: Effect of  $n_f$  on  $V_p/V_{p(Theory)}$

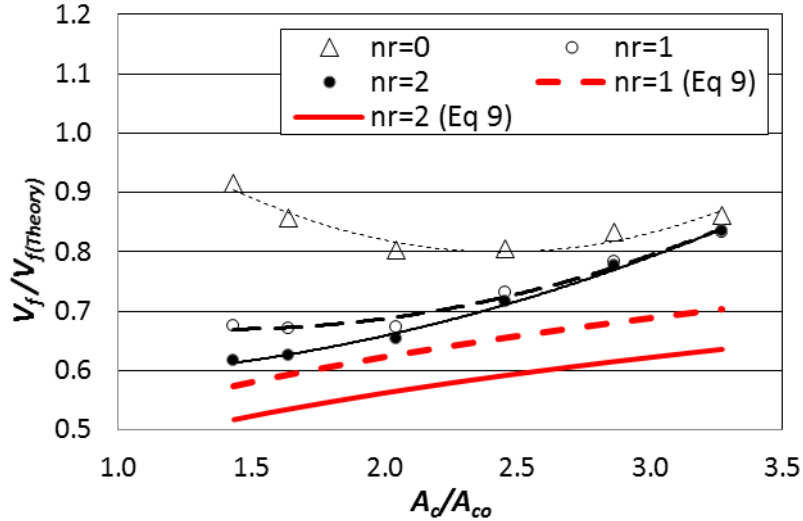


Figure 20: Effect of  $A_c/A_{co}$  on  $V_f/V_{f(Theory)}$

Fig 21 showed that  $V_f/V_{f(Theory)}$  was proportional to  $I_c/I_b$  in CR-SPSWs and SPSWs, however, the use of restrainers reduced the base shear supported by boundary frame elements in CR-SPSWs. Fig 22 showed that  $V_f/V_{f(Theory)}$  increased progressively with  $F_{yp}/F_{yf}$  in SPSWs compared to identical CR-SPSWs. Therefore, it was possible to increase  $F_{yp}/F_{yf}$  in CR-SPSW to 0.8 without increasing  $V_f/V_{f(Theory)}$  more than 0.7. However,  $F_{yp}/F_{yf}$  should not exceed 0.6 to limit  $V_f/V_{f(Theory)}$  in SPSWs to 0.7. Therefore the use of column restrainers allowed the use of in-fill plate with higher yield strength without affecting the increasing internal forces in boundary frame elements. Similarly, Figs 23 and 24 revealed that the use of column restrainers allowed the increase of in-fill plate area relative to horizontal and vertical boundary elements without increasing base shear supported by frame elements. In SPSWs,  $t_p h_p/A_b$  and  $t_p L_p/2A_c$  should not exceed 0.23 and 0.15; respectively to keep  $V_f/V_{f(Theory)}$  below 0.7. However, in CR-SPSW, it was possible to bound  $V_f/V_{f(Theory)}$  below 0.7 at  $t_p h_p/A_b$  and  $t_p L_p/2A_c$  of 0.33 and 0.23; respectively. Fig 25 showed that the use of column restrainers reduced the rapid increase of  $V_f/V_{f(Theory)}$  when  $n_f$  increased without respective increase in  $A_c$  and/or  $I_c$ .

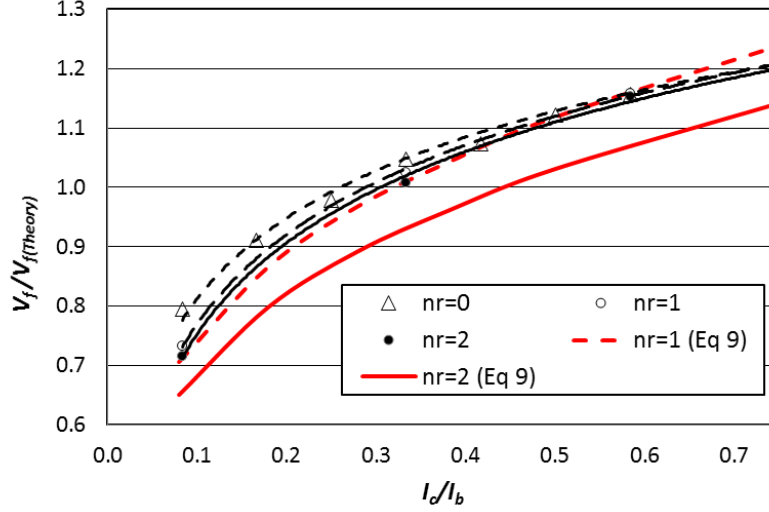


Figure 21: Effect of  $l_c/l_b$  on  $V_f/V_{f(Theory)}$

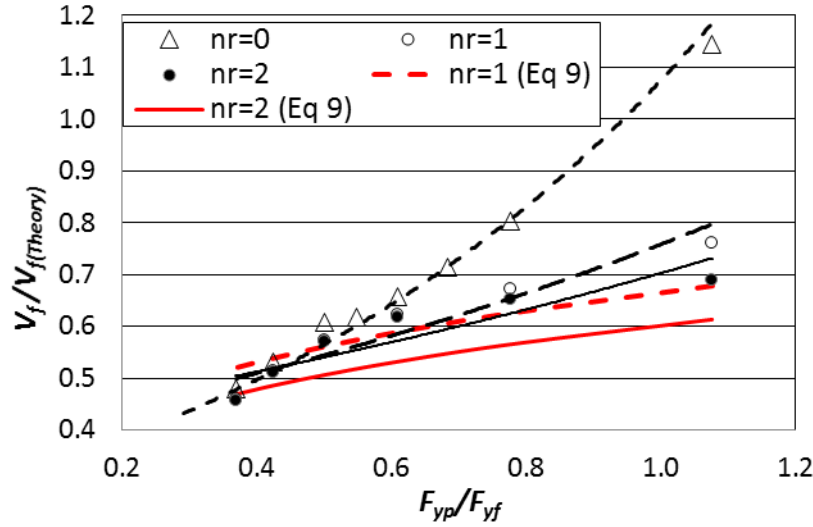


Figure 22: Effect of  $F_{yp}/F_{yf}$  on  $V_f/V_{f(Theory)}$

## 6. Shear Strength and Design Recommendations of CR-SPSWs

Discrepancies between numerical and theoretical results of  $V_p$  and  $V_f$  were mainly attributed to complex interaction of in-fill plate, restrainers and boundary frame elements. Therefore, it was decided to express the ultimate shear strength of CR-SPSW,  $V_s$ , as follows:

$$V_s = \eta_p V_{p(Theory)} + \eta_f V_{f(Theory)} \quad (7)$$

where  $\eta_p$  and  $\eta_f$  are modification factors to account for interaction of the components of CR-SPSW. The factors  $\eta_p$  and  $\eta_f$  were obtained by regression analysis of numerical results of  $V_p/V_{p(Theory)}$  and  $V_f/V_{f(Theory)}$ ; respectively as follows:

$$\eta_p = \left[ \frac{(n_r+1)}{n_f} \right]^{0.07} \left[ \frac{A_c F_{yf}}{A_{co} F_{yp}} \right]^{0.04} \leq 1.05 \quad (8)$$

$$\eta_f = \left[ \frac{n_f F_{yp}}{F_{yf}} \right]^{0.5} \left[ \frac{A_c t_p h_p l_c}{A_{co} (n_r+1) A_b l_b} \right]^{0.25} \quad (9)$$

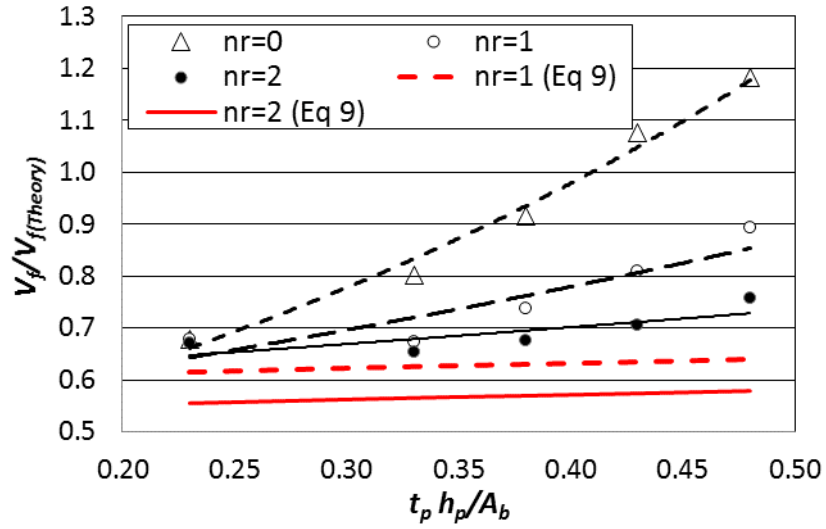


Figure 23: Effect of  $t_p h_p / A_b$  on  $V_f / V_f(\text{Theory})$

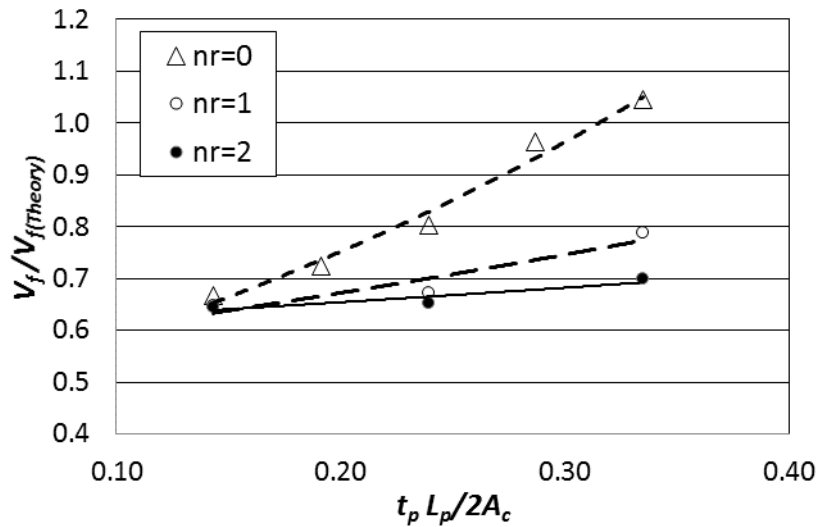


Figure 24: Effect of  $t_p L_p / 2A_c$  on  $V_f / V_f(\text{Theory})$

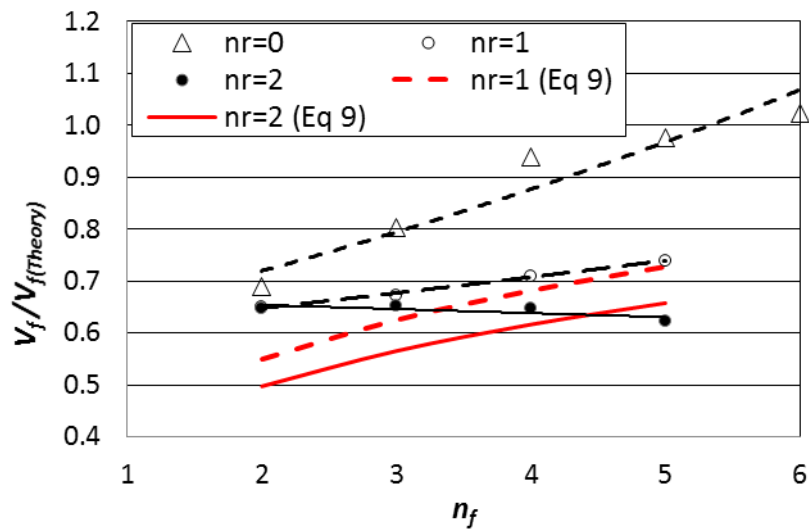


Figure 25: Effect of  $n_f$  on  $V_f / V_f(\text{Theory})$



The plate modification factor,  $\eta_p$ , was allowed to exceed unity with an upper bound of 1.05 to account for values of  $V_p/V_{p(Theory)}$  that exceeded unity due to increase of the angle  $\alpha$  when column restrainers were used. The regression coefficient of the power models of  $\eta_p$  and  $\eta_f$  were 0.86 and 0.93; respectively. Scatter diagrams of  $\eta_p V_{p(Theory)}/V_p$  and  $\eta_f V_{f(Theory)}/V_f$  for the eighty two CR-SPSWs solved herein revealed that the proposed expressions were acceptable and predicted numerical results with an average value of 0.98 and 0.85; respectively. Figs 14, 16 and 19 showed that the proposed expression of  $V_p = \eta_p V_{p(Theory)}$  was compatible with numerical results. Figs 20 to 23 and 25 showed that the proposed expression of  $V_f = \eta_f V_{f(Theory)}$  was compatible with numerical results.

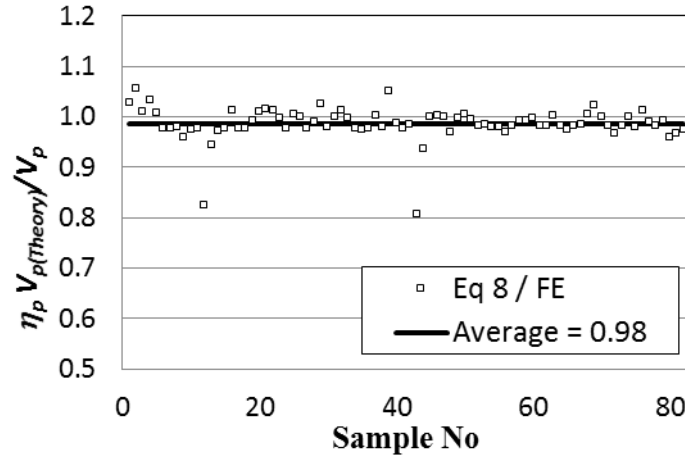


Figure 26: Comparison of  $\eta_p$  to numerical results

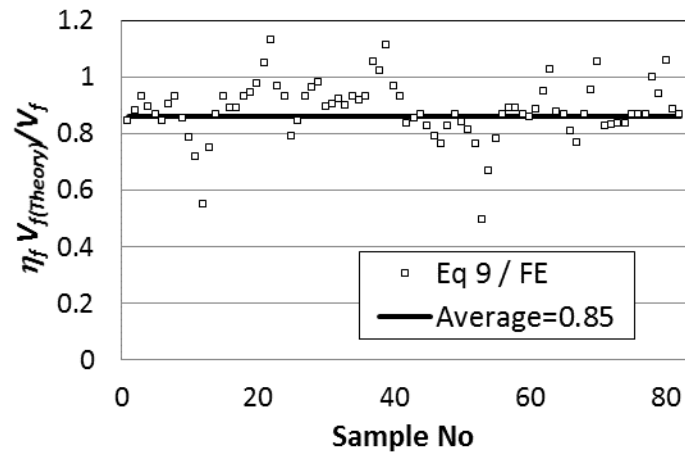


Figure 27: Comparison of  $\eta_f$  to numerical results

Based on the work presented herein and current design specifications (AISC 2005, CSA 2005), it was recommended to design CR-SPSWs to support gravity loads and transverse loads corresponding to full tensile strength of in-fill plate (i.e.  $V_p/V_{p(Theory)} \geq 1.0$  or  $\eta_p \geq 1.0$ ) and less than 70% of base shear corresponding to uniform yielding mechanism (i.e.  $V_f/V_{f(Theory)} \leq 0.70$  or  $\eta_f \leq 0.7$ ). Eqs (8) and (9) could be utilized to verify that the dimensions and material properties of CR-SPSWs satisfied such conditions based on the assumptions adopted herein (i.e. identical in-fill plate thickness and columns in all floors,  $A_b$  of top beam is 4 times that of intermediate beams,  $I_b$  of top beam is 1.33 times that of intermediate beams, and beams are rigidly connected to beams). Based on numerical results, it was revealed that  $A_c/A_{co}$  and  $F_{yp}/F_{yf}$  were indeed

influential on the behavior of CR-SPSWs. Therefore, it was recommended to proportion the wall such that;  $1.5 < A_c/A_{co} \leq 2.0$  (see Figs 14 and 20), and  $F_{yp}/F_{yf} \leq 0.80$  (see Figs 16 and 22).

## 7. Summary and Conclusions

In this work, push-over analysis of more than eighty CR-SPSWs with wide variety of dimensions and material properties was conducted using the finite element method. The numerical model was verified by comparison to test results published in literature. Numerical results were used to establish a mathematical expression for the ultimate shear strength of CR-SPSWs and establish design recommendations for columns and column-restrainers.

Based on the work conducted herein, the following was concluded:

- Use of column restrainers in SPSWs reduced column in-ward deflections, reduced base shear supported by boundary elements at a given drift, reduced rigidity requirements of boundary frame elements to achieve full yielding of in-fill plate, and prevented plastic hinges in first story columns far from base connection.
- Use of column restrainers in SPSWs accelerated full yielding of in-fill plate at a drift not more than 2.5%, allowed the increase of in-fill plate thickness and strength without increasing base shear supported by boundary frame elements, and slightly increased angle of inclination of diagonal tension forces in the in-fill plate with the vertical.
- Based on design assumptions adopted herein and numerical results, a mathematical expression for ultimate shear strength of CR-SPSWs was established. The model described the portion of base shear supported by in-fill plate and boundary frame elements.
- In order to achieve full yielding of in-fill plate and bound base shear supported by boundary frame elements less than 70% of that corresponding to uniform yielding mechanism, it was recommended to proportion CR-SPSWs such that  $1.5 < A_c/A_{co} \leq 2.0$  and  $F_{yp}/F_{yf} \leq 0.80$ .
- Column restrainers should be designed to support axial force resulting from horizontal component of diagonal tension forces on columns based on full yielding of in-fill plate assuming out-of-plane buckling length of not less than  $0.75 L_p$ .

## References

- Amer, M.A. (2014), "Analysis and Design of Steel Plate Shear Walls", *PhD Dissertation*, Cairo University, Faculty of Engineering.
- Berman, J.W. and Bruneau, M. (2003), "Experimental Investigation of Light-gauge Steel Plate Shear Walls for the Seismic Retrofit of Buildings", *Technical report MCEER-03-0001*, Multidisciplinary Center for Earthquake Engineering Research, Buffalo, N.Y., USA.
- American Institute for Steel Construction, ANSI/AISC 341-05 (2005), "Seismic Provisions for Structural Steel Buildings", Chicago, IL, USA.
- Canadian Standards Association, CAN/CSA-S16-01 (2001), "Limit States Design of Steel Structures", Toronto, Canada.
- Datsfan, M. and Driver, R.G. (2008), "Flexural Stiffness Limits For Frame Members of Steel Plate Shear Wall Systems", *Proceedings of Annual Stability Conference*, Structural Stability Research Council, Nashville, TN, USA.
- Park, H. G., Kwack, J. H., Jeon, S. W., Kim, W. K. and Choi, I. R. (2007), "Framed Steel Plate Wall Behavior under Cyclic Lateral Loading", *Journal of Structural Engineering*, 133(3), 378-388.
- Choi, I. R. and Park, H. G. (2008), "Ductility and Energy Dissipation Capacity of Shear-Dominated Steel Plate Walls", *ASCE Journal of Structural Engineering*, 134(9), 1495-1507.

- Choi, I. R. and Park, H. G. (2009), "Steel Plate Shear Walls with Various Infill Plate Designs" *ASCE Journal of Structural Engineering*, 135(7), 785-796.
- Driver, R. G., Kulak, G.L., and Kennedy, G.J. (1997), "Seismic Behavior of Steel Plate Shear Walls", *Structural Engineering Report no. 215*, University of Alberta, Canada.
- Behbahani, M. R., and Grondin, G.Y., and Elwi, A.E. (2003), "Experimental and Numerical Investigation of Steel Plate Shear Wall", *Structural Engineering Report no. 254*, University of Alberta, Canada.
- Chao, H. L., Tsia, K. C., Lin, C. H., Tsai, C. H., and Yu, Y. J. (2010), "Cyclic tests of four two-story narrow steel plate shear walls-Part 1: Analytical studies and specimen design" *Earthquake Engineering and Structural Dynamics*, 39, 775-799.
- Chao, H. L., Tsai, K. C., Lin, C. H., and Chen, P. C. (2010), "Cyclic tests of four two-story narrow steel plate shear walls-Part 2: Experimental results and design implications" *Earthquake Engineering and Structural Dynamics*, 39, 801-826.
- Desalvo, G.J., and Gorman, R.W. (1989), "ANSYS User's Manual", Swanson Analysis Systems, Houston, PA.
- Machaly, E.B., Safar, S. S. and Amer, M.A. (2014), "Finite Element Analysis of Light Gauge Steel Plate Shear Walls", *Proceedings of the Eleventh International Conference on Computational Structures Technology*, Civil-Comp Press, Paper 8.